# (Extreme) Tidal Disruption Events as probes of Nuclear Star Cluster

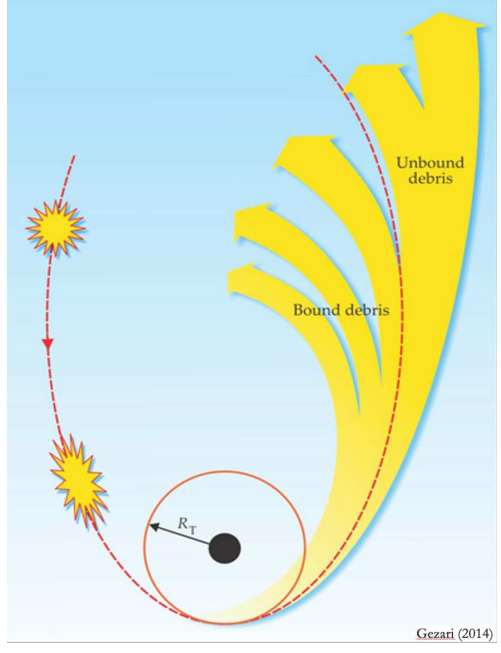


Vladimír Karas

Astronomical Institute, Czech Academy of Sciences, Prague

# NSC-gas interaction

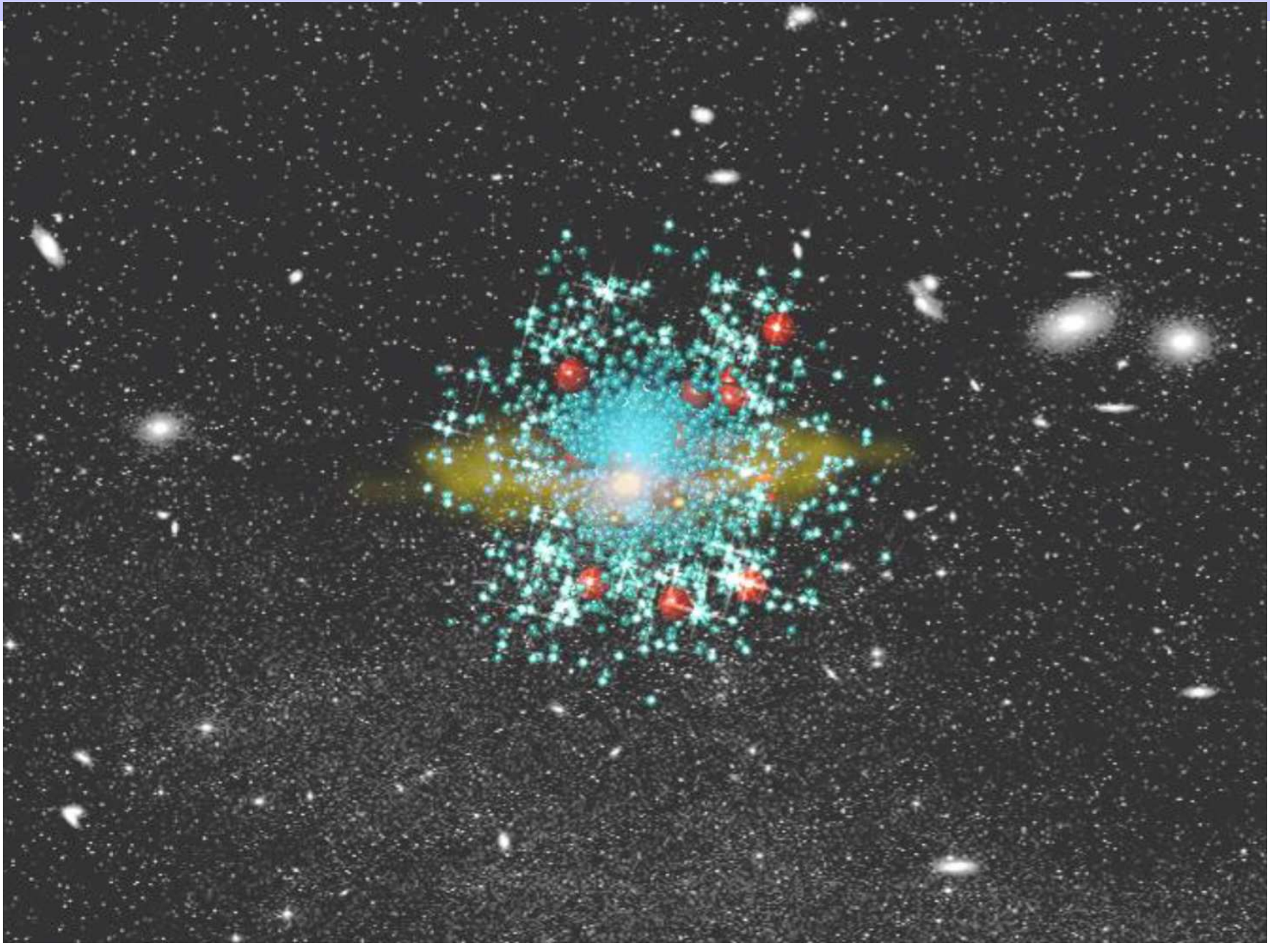

# Star-disc interaction

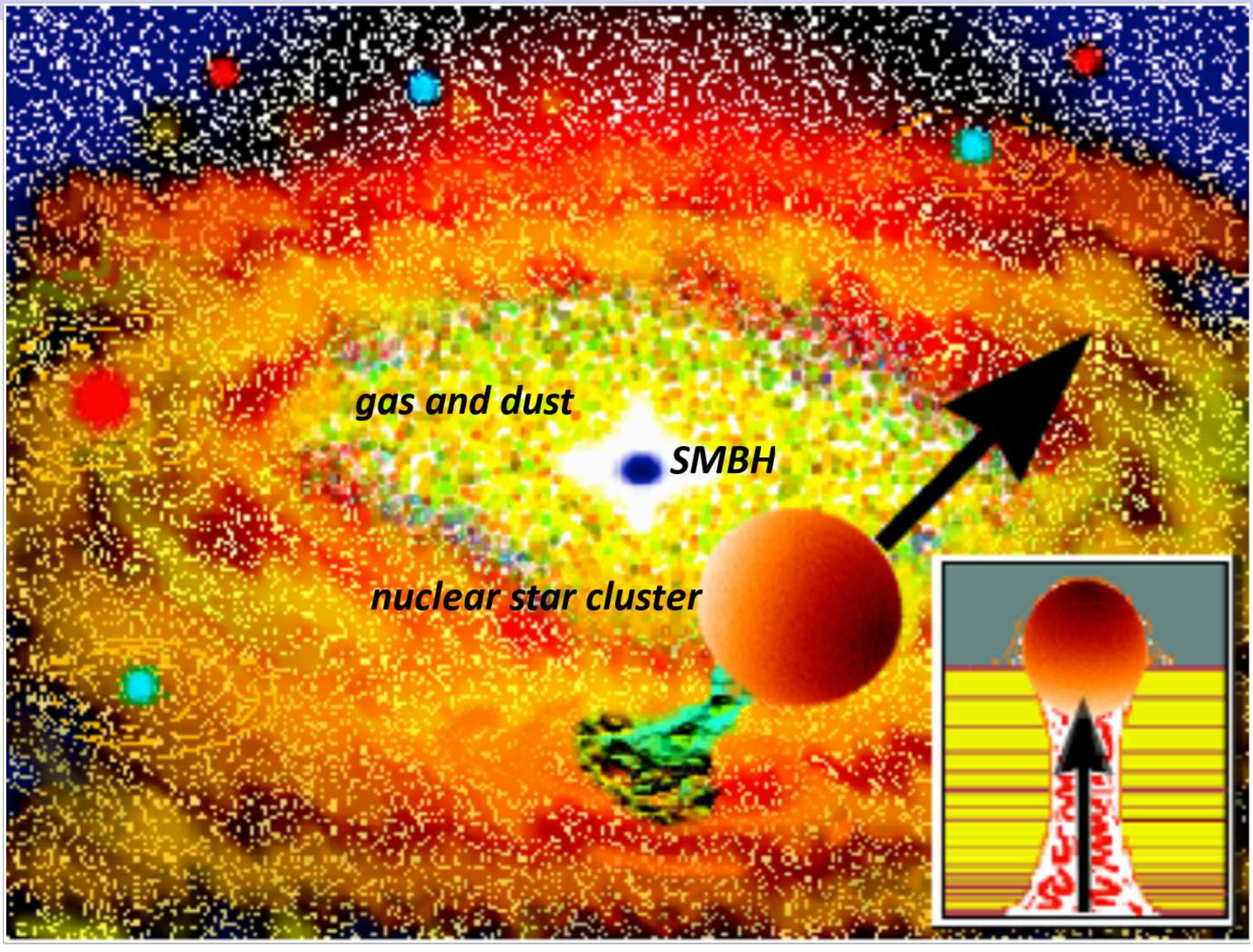

# Star-disc orbital elements

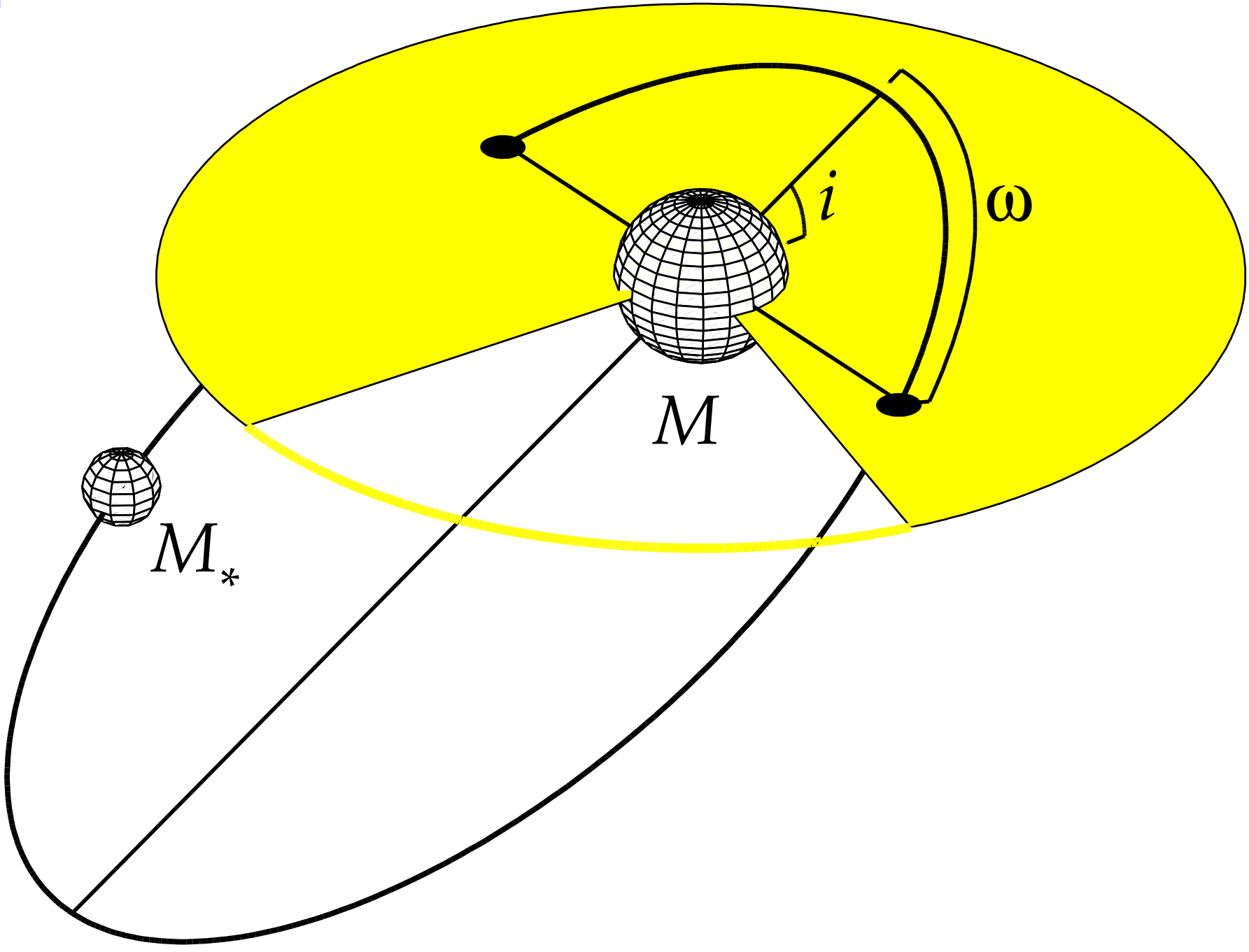

# Two-body Hamiltonian

Carthesian coordinates:

$$\mathcal{H} = \frac{1}{2}\left(v_1^2 + v_2^2 + v_3^2\right) - \frac{\mathcal{G}\,(m_0 + m_1)}{\sqrt{x_1^2 + x_2^2 + x_3^2}}$$

Delaunay variables:

$$\mathcal{H} = -\frac{\mathcal{G}^2 (m_0 + m_1)^2}{2L^2}$$

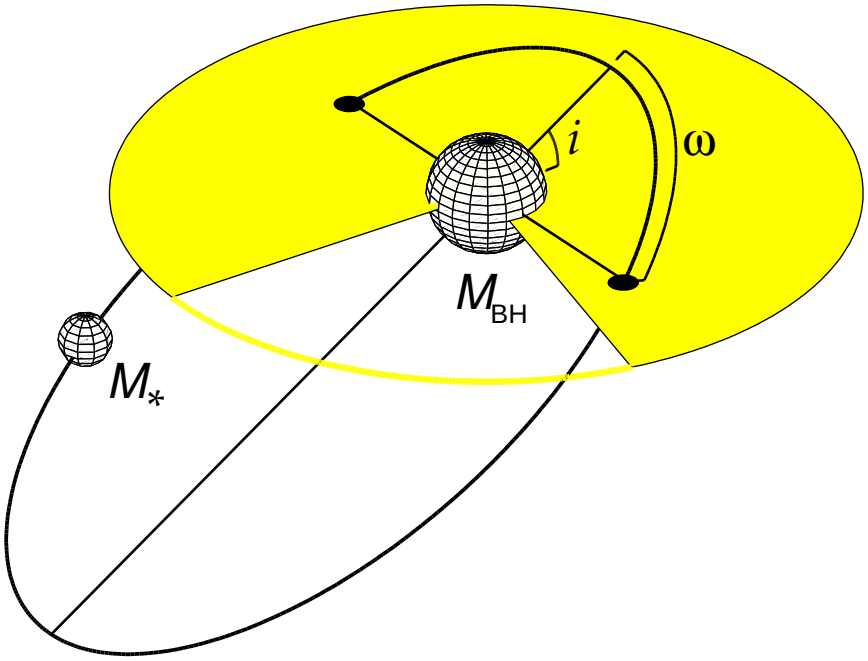


$$L = \sqrt{\mathcal{G}(m_0 + m_1)a} \qquad l = M$$
$$G = L\sqrt{1 - e^2} \qquad g = \omega$$
$$H = G\cos i \qquad h = \Omega$$

# Model

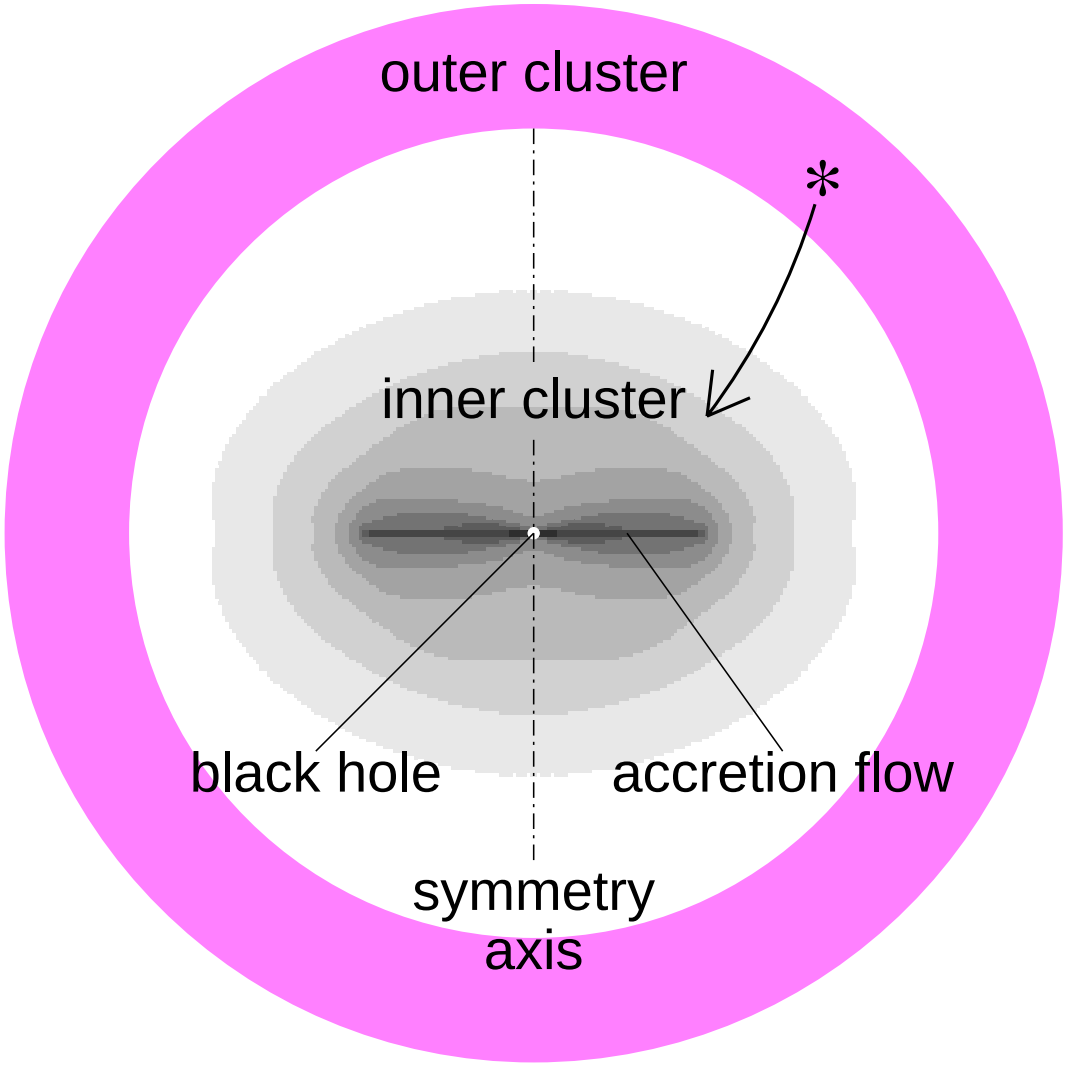


- Black hole
  $M_{\rm BH} \approx 10^3 - 10^8 M_\odot$
- Accretion flow
  $\Sigma_{\rm d} \propto r^{\rm s}$
  $R_{\rm d} \approx 10^4 R_{\rm g} \approx 0.1\,{\rm pc}$
- 'Outer' cluster
  $n(r) = n_0 (r/r_{\rm h})^{-7/4}$
  $r_{\rm h} \approx 10\,{\rm pc}$
  $n_0 \approx 10^6 - 10^8 {\rm pc}^{-3}$
- 'Inner' cluster…

# *Kozai–Lidov mechanism*

- evolution of a hiearchical triple system $m_0 > m_1 > m_2$

  Lidov 1961: Earth > Moon > satellite

  Kozai 1962: Sun > Jupiter > asteroid

- secular evolution of the orbital elements $e$, $i$ and $\omega$
- 'averaging' technique of the Hamiltonian perturbation theory allows to get rid of 'fast' variable (mean anomaly)
- integrals of motion: $a$, $C_1 \equiv \sqrt{1-e^2}\,\cos i$ and $\bar{V}_\mathrm{d}$
- motion of a star in the gravitational field of the central mass and an axisymmetric perturbation (ring, torus, disc...)

# Kozai equations

Newtonian framework

$$T_{\rm K}\sqrt{1-e^2}\,\frac{{\rm d}i}{{\rm d}t} = -5e^2\sin i\,\cos i\,\sin\omega\,\cos\omega$$

$$T_{\rm K}\sqrt{1-e^2}\,\frac{{\rm d}e}{{\rm d}t} = 5e(1-e^2)\sin^2 i\,\sin\omega\,\cos\omega$$

$$T_{\rm K}\sqrt{1-e^2}\,\frac{{\rm d}\omega}{{\rm d}t} = 2(1-e^2)+5(e^2-\sin^2 i)\sin^2\omega$$

$$T_{\rm K} \equiv \frac{4}{3}\frac{M_{\rm BH}}{M_{\rm d}}\left(\frac{R_{\rm d}}{a}\right)^3 P$$

# $\bar{V}_{\rm d}$ = const., *perturbation potential for a disc*

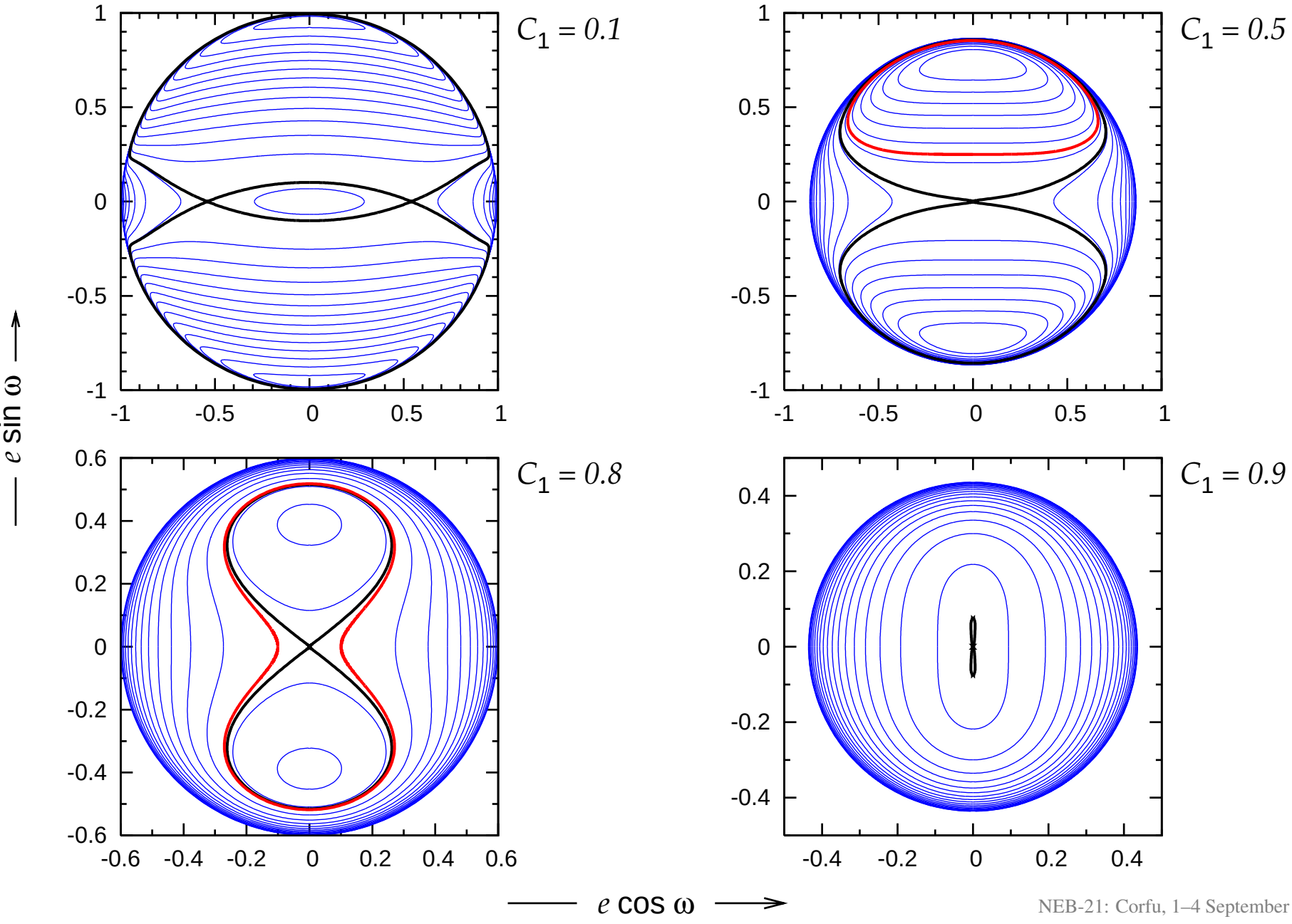

# *Damping effect of the relativistic pericentre advance*

- Characteristic timescales:

$$T_{\mathrm{K}} = \frac{4}{3}\frac{M_{\mathrm{BH}}}{M_{\mathrm{d}}}\left(\frac{R_{\mathrm{d}}}{a}\right)^{3} P \qquad \text{vs.} \qquad T_{\mathrm{E}} = \frac{1}{3}\frac{a(1-e^{2})}{R_{\mathrm{g}}} P$$

- Kozai oscillations are suppressed for

$$a < a_{\mathrm{min}} \approx \left(\frac{M_{\mathrm{BH}}}{M_{\mathrm{d}}}\right)^{2} \left(\frac{R_{\mathrm{d}}}{R_{\mathrm{g}}}\right)^{6/7} \left(\frac{R_{\mathrm{min}}}{R_{\mathrm{g}}}\right)^{-1/7} R_{\mathrm{g}}$$

*... prominent effect in case of extreme relativistic TDE* *(Karas & Šubr, 2007, A&A)*

# *Damping effect of the relativistic pericentre advance*

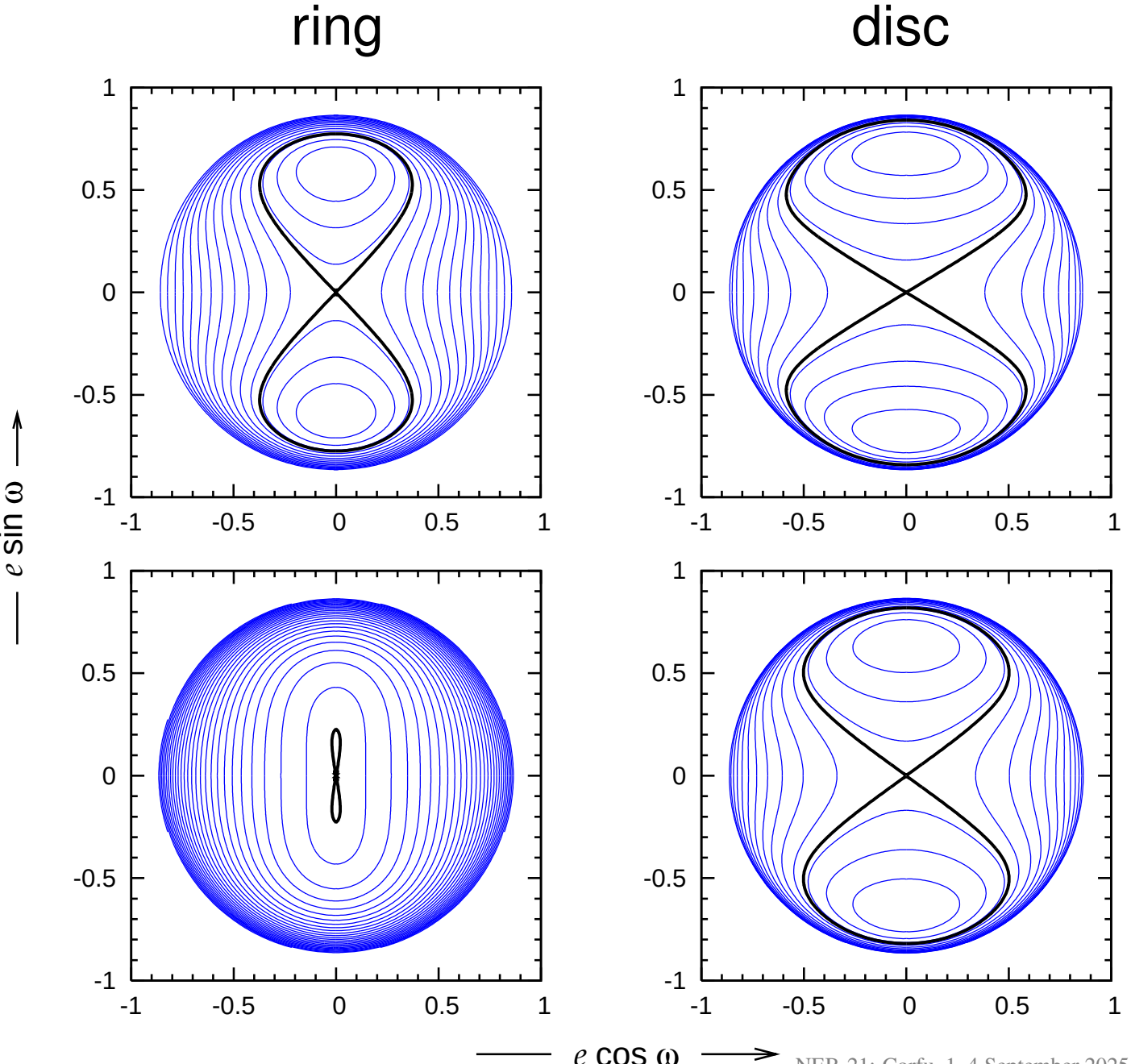

# *Effect of an extended star cluster*

Stellar cusp in the sphere of influence of the central black hole

- Bahcall & Wolf (1976): $\rho(r) \propto r^{-7/4}$
- Galactic centre:

$$\rho(r) \approx 1.2 \times 10^6 \left(\frac{r}{0.4\mathrm{pc}}\right)^{-\alpha} M_\odot\,\mathrm{pc}^{-3}$$

$$\alpha = \begin{cases} 1.4 & r \lesssim 0.4\mathrm{pc} \\ 2.0 & r \gtrsim 0.4\mathrm{pc} \end{cases}$$

$$V_c(r) \propto \begin{cases} r^{2-\alpha} & \alpha < 2 \\ \ln(r) & \alpha = 2 \end{cases}$$

# *Tidal disruptions*

- enhanced tidal disruptions due to the eccentricity oscillations
- supply of gas for accretion discs; food for black holes

$$R_{\rm t} \;=\; \left(\frac{M_{\rm BH}}{M_*}\right)^{1/3} R_* \;=\; 47\left(\frac{M_{\rm BH}}{10^6 M_\odot}\right)^{-2/3}\left(\frac{M_*}{M_\odot}\right)^{-1/3}\left(\frac{R_*}{R_\odot}\right) R_{\rm g}$$

- characteristic radius of the stellar cluster $\sim 10^6 R_{\rm g} \implies$ extreme eccentricities needed
- $\mathcal{F}(R_{\rm min})$: fraction of stars from an ensemble with given (initial) distribution of orbital elements $D_{\rm f}(a, e, i, \omega)$ that pass the centre within $R_{\rm min}$.

# Fractional probabilities

$$\mathcal{F}_1(R_{\rm min};a) \equiv \frac{1}{D_1}\int_0^1 {\rm d}C_1 \int_0^{\sqrt{1-C_1^2}} {\rm d}e \int_0^{2\pi} {\rm d}\omega\ \Theta(e_{\rm max}-e_{\rm min}) D_{\rm f}(a,C_1,e,\omega)$$

$$\mathcal{F}(R_{\rm min}) \equiv \int_{a_{\rm min}}^{a_{\rm max}} {\rm d}a \int_0^1 {\rm d}C_1 \int_0^{\sqrt{1-C_1^2}} {\rm d}e \int_0^{2\pi} {\rm d}\omega\ \Theta(e_{\rm max}-e_{\rm min}) D_{\rm f}(a,C_1,e,\omega)$$

where

$$D_1(a) \equiv \int_0^1 {\rm d}C_1 \int_0^{\sqrt{1-C_1^2}} {\rm d}e \int_0^{2\pi} {\rm d}\omega\ D_{\rm f}(a,C_1,e,\omega)$$

$$e_{\rm min} \equiv 1 - R_{\rm min}/a$$

$$e_{\rm max} \equiv e_{\rm max}(a,C_1,e,\omega)$$

# Analytical estimates

$$D_{\rm f}(a,i,e,\omega) = D_0\, a^{1/4} e \cos i \simeq D_0'\, a^{1/4} \frac{e}{\sqrt{1-e^2}}$$

- /w central potential:

$$\begin{aligned} \mathcal{F}(R_{\rm min}) &\approx 10 R_{\rm min}/a_{\rm max} \\ \mathcal{F}_1(R_{\rm min};a) &= 2R_{\rm min}/a - R_{\rm min}^2/a^2 \end{aligned}$$

- /w Kozai:

$$\begin{aligned} \mathcal{F}(R_{\rm min}) &\approx \tfrac{10}{3}\sqrt{2R_{\rm min}/a_{\rm max}} \\ \mathcal{F}_1(R_{\rm min};a) &\approx 2\sqrt{2R_{\rm min}/a} \end{aligned}$$

# Exemplary model

- mass-sigma relation: $\sigma \approx 20\,(M_{\rm BH}/10^4 M_\odot)^{1/4}\,{\rm km\,s^{-1}}$
- characteristic radius of the star cluster: $R_{\rm h} = GM_{\rm BH}/\sigma^2$
- $R_{\rm d} = R_{\rm h}\,,\ 0.04R_{\rm h} \le a \le 0.4R_{\rm h}$
- $M_{\rm d} = 0.01M_{\rm BH}\,,\ M_{\rm c} = M_{\rm BH}\,,\ M_* = M_\odot\,,\ R_* = R_\odot$

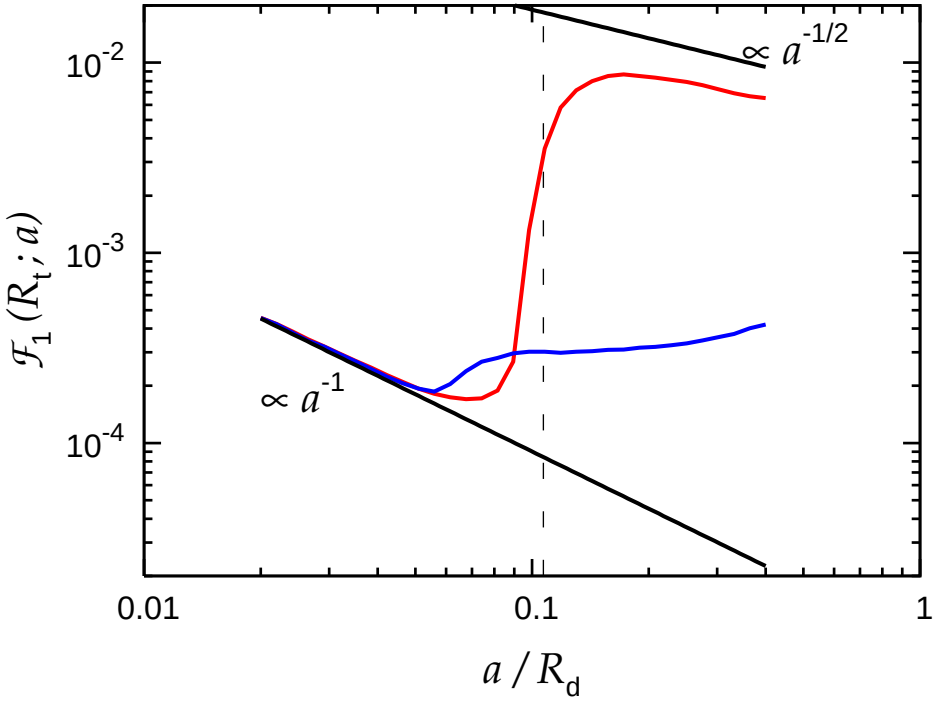


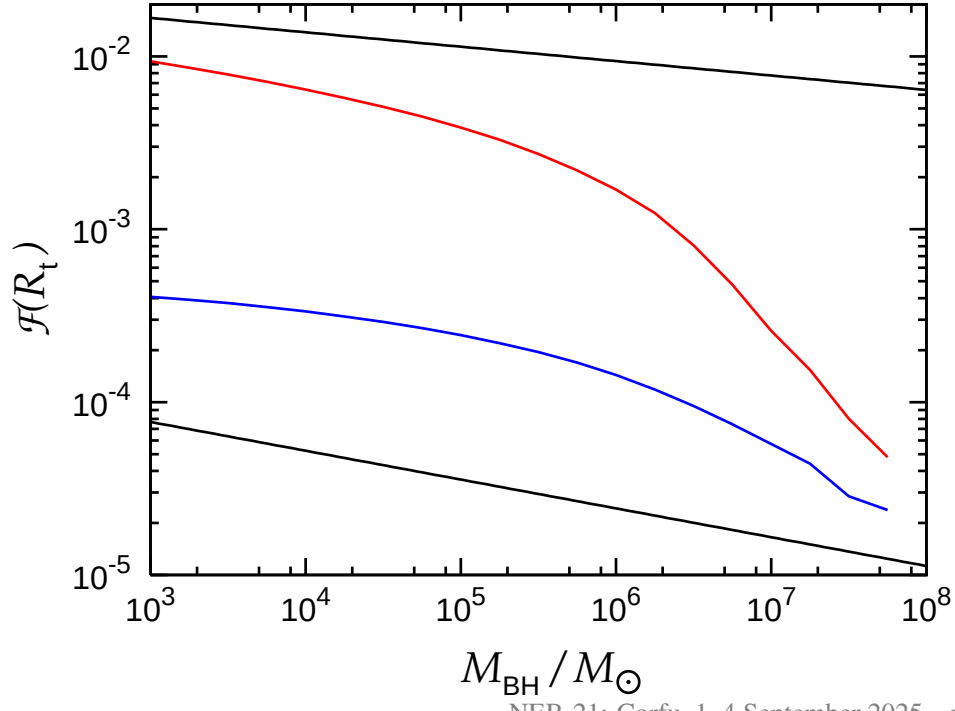

# *In the Galactic centre*

molecular torus (ring):

$$M_\mathrm{d} = 0.1 M_\mathrm{BH}$$
$$R_\mathrm{d} = 1.6\,\mathrm{pc}$$

star cluster:

$$\rho(r) \propto r^{-1.75}$$
$$M_\mathrm{c}(1.6\mathrm{pc}) = M_\mathrm{BH}$$

---

$$\mathcal{F}(R_\mathrm{t}) \approx 3 \times 10^{-4}$$
$$N \approx 100$$

(clockwise) stellar disc:

$$M_\mathrm{d} = 0.01 M_\mathrm{BH}$$
$$R_\mathrm{in} = 0.03\,\mathrm{pc}$$
$$R_\mathrm{out} = 0.3\,\mathrm{pc}$$
$$\Sigma(r) \propto r^{-2}$$

star cluster:

$$\rho(r) \propto r^{-1.4}$$
$$M_\mathrm{c}(0.4\mathrm{pc}) = 0.2 M_\mathrm{BH}$$

---

$$\mathcal{F}(R_\mathrm{t}) \approx 2 \times 10^{-3}$$
$$N \approx 100$$

# EMRI vs. TDE vs. QPE

**EMRI + TDE = QPE: Periodic X-Ray Flares from Star–Disk Collisions in Galactic Nuclei**

The Astrophysical Journal, 957:34 (19pp), 2023 November 1

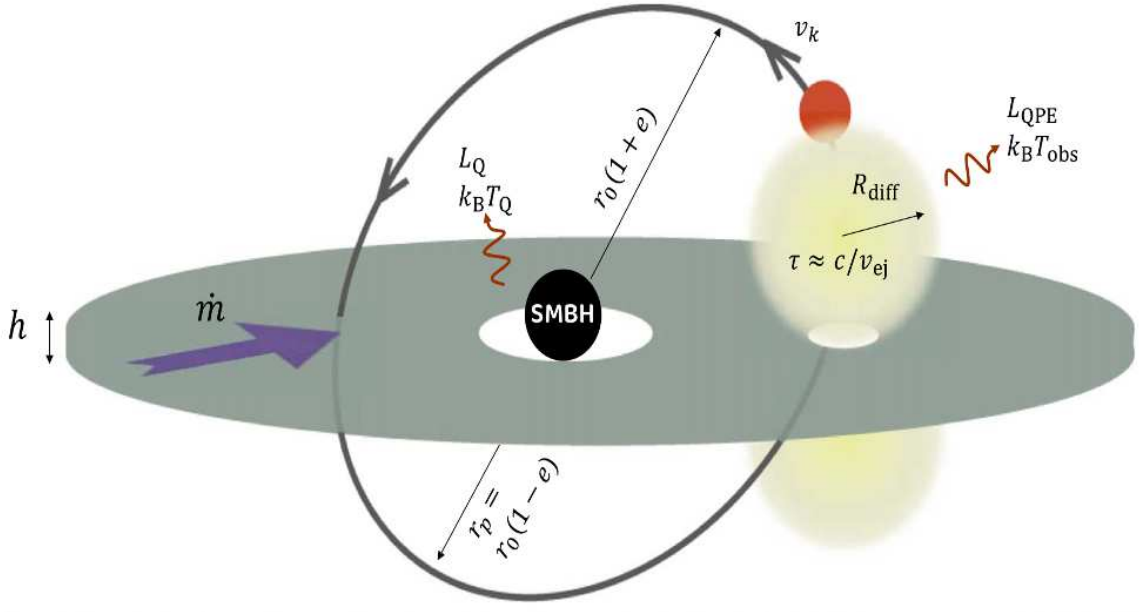


**Figure 1.** Schematic view of our model. A star orbits an SMBH that is accreting matter through a thin disk of scale height $h$ at a rate $\dot{m}$. Due to the inclined orbital plane, the star impacts the disk twice per orbit, carving a hole through the disk and ejecting an optically thick cloud of material expanding above and below the disk plane. As the ejecta expands and cools, photons begin to diffuse out, and the light curve peaks once the optical depth drops below $c/v_{\rm ej}$, where $v_{\rm ej} \sim v_{\rm K}$ is the ejecta velocity imparted by the colliding star. The inner regions of the disk dominate the soft quiescent emission seen between the collision-powered flares.

The Astrophysical Journal, 983:40 (26pp), 2025 April 10 Vurm, Linial, & Metzger

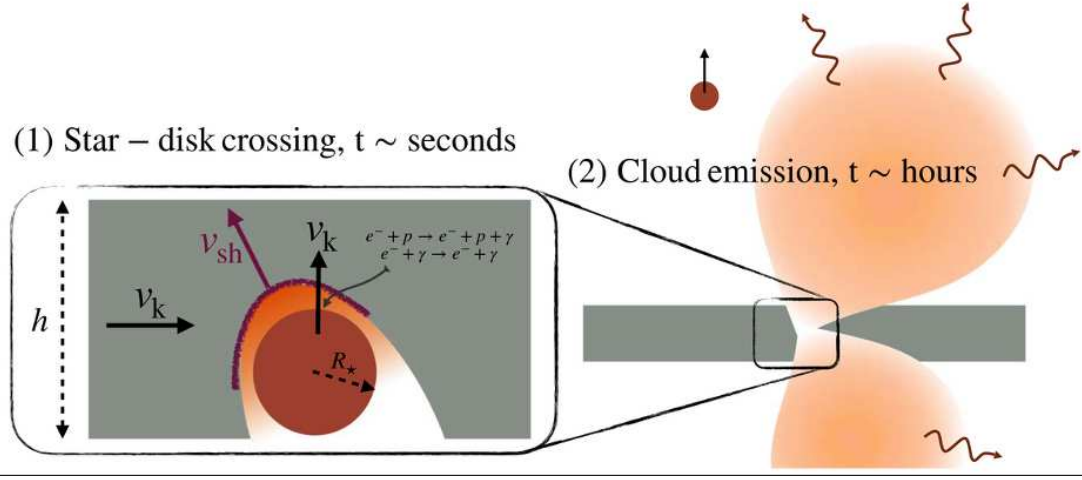

# EMRI vs. TDE vs. QPOut

Pasham *et al.*, *Sci. Adv.* **10**, eadj8898 (2024) 27 March 2024

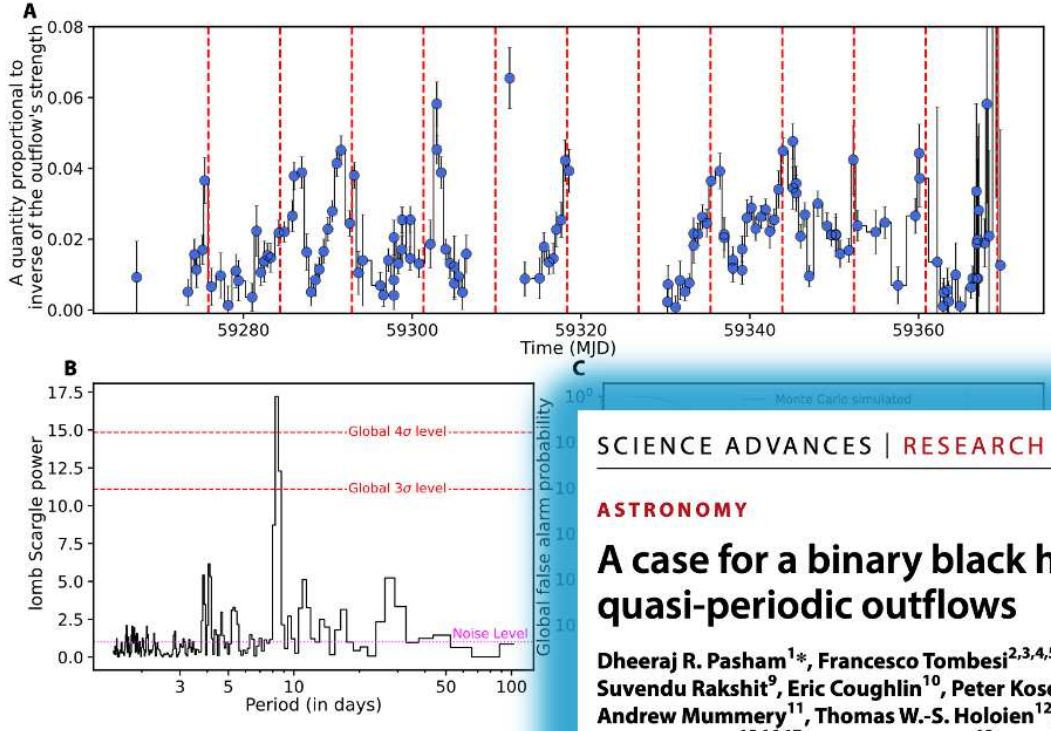


**Fig. 2. Summary of ASASSN-20qc's timing analysis.** (**A**) ASASSN-20qc's ODR versus tim
1.00-keV (outflow) and 0.3- to 0.55-keV (continuum) bands. A lower ODR value implies a st
rated by 8.5 days. (**B**) Lomb-Scargle periodogram (LSP) of the ODR. The strongest signal is
alarm probabilities as per (*6*). The noise in the periodogram is consistent with white with a
consistent with white noise" section). (**C**) Global (trials-accounted) false alarm probability.
als and Methods, "ODR timing analysis" section). The global statistical significance of the 8.

SCIENCE ADVANCES | RESEARCH ARTICLE

ASTRONOMY

## A case for a binary black hole system revealed via quasi-periodic outflows


**Dheeraj R. Pasham[1]*, Francesco Tombesi[2,3,4,5,6], Petra Suková[7], Michal Zajaček[8], Suvendu Rakshit[9], Eric Coughlin[10], Peter Kosec[1,23], Vladimír Karas[7], Megan Masterson[1], Andrew Mummery[11], Thomas W.-S. Holoien[12], Muryel Guolo[13], Jason Hinkle[14], Bart Ripperda[15,16,17], Vojtěch Witzany[18], Ben Shappee[14], Erin Kara[1], Assaf Horesh[19], Sjoert van Velzen[20], Itai Sfaradi[19], David Kaplan[21], Noam Burger[19,22], Tara Murphy[23,24], Ronald Remillard[1], James F. Steiner[25], Thomas Wevers[26], Riccardo Arcodia[1], Johannes Buchner[27], Andrea Merloni[27], Adam Malyali[27], Andy Fabian[28], Michael Fausnaugh[1], Tansu Daylan[29], Diego Altamirano[30], Anna Payne[14], Elizabeth C. Ferraraa[5,6,31]**



**Binaries containing a compact object orbiting a supermassive black hole are thought to be precursors of gravitational wave events, but their identification has been extremely challenging. Here, we report quasi-periodic variability in x-ray absorption, which we interpret as quasi-periodic outflows (QPOuts) from a previously low-luminosity active galactic nucleus after an outburst, likely caused by a stellar tidal disruption. We rule out several models based on observed properties and instead show using general relativistic magnetohydrodynamic simulations that QPOuts, separated by roughly 8.3 days, can be explained with an intermediate-mass black hole secondary on a mildly eccentric orbit at a mean distance of about 100 gravitational radii from the primary. Our work suggests that QPOuts could be a new way to identify intermediate/extreme-mass ratio binary candidates.**

# EMRI vs. TDE

The Astrophysical Journal, 909:62 (19pp), 2021 March 1 https://doi.org/10.3847/1538-4357/abd9c6


## First Observed Interaction of the Circumstellar Envelope of an S-star with the Environment of Sgr A*

Florian Peißker[1], Basel Ali[1], Michal Zajaček[2,1], Andreas Eckart[1,3], S. Elaheh Hosseini[1,3], Vladimír Karas[4], Yann Clénet[5], Nadeen B. Sabha[6], Lucas Labadie[1], and Matthias Subroweit[1]
[1] I. Physikalisches Institut der Universität zu Köln, Zülpicher Str. 77, D-50937 Köln, Germany; Peissker@ph1.uni-koeln.de
[2] Center for Theoretical Physics, Al. Lotników 32/46, 02-668 Warsaw, Poland
[3] Max-Plank-Institut für Radioastronomie, Auf dem Hügel 69, D-53121 Bonn, Germany
[4] Astronomical Institute, Czech Academy of Sciences, Boční II 1401, CZ-14100 Prague, Czech Republic
[5] LESIA, Observatoire de Paris, Université PSL, CNRS, Sorbonne Université, Université de Paris, 5 place Jules Janssen, F-92195 Meudon, France
[6] Institut für Astro- und Teilchenphysik, Universität Innsbruck, Technikerstr. 25, A-6020 Innsbruck, Austria
*Received 2020 November 24; revised 2021 January 4; accepted 2021 January 6; published 2021 March 4*

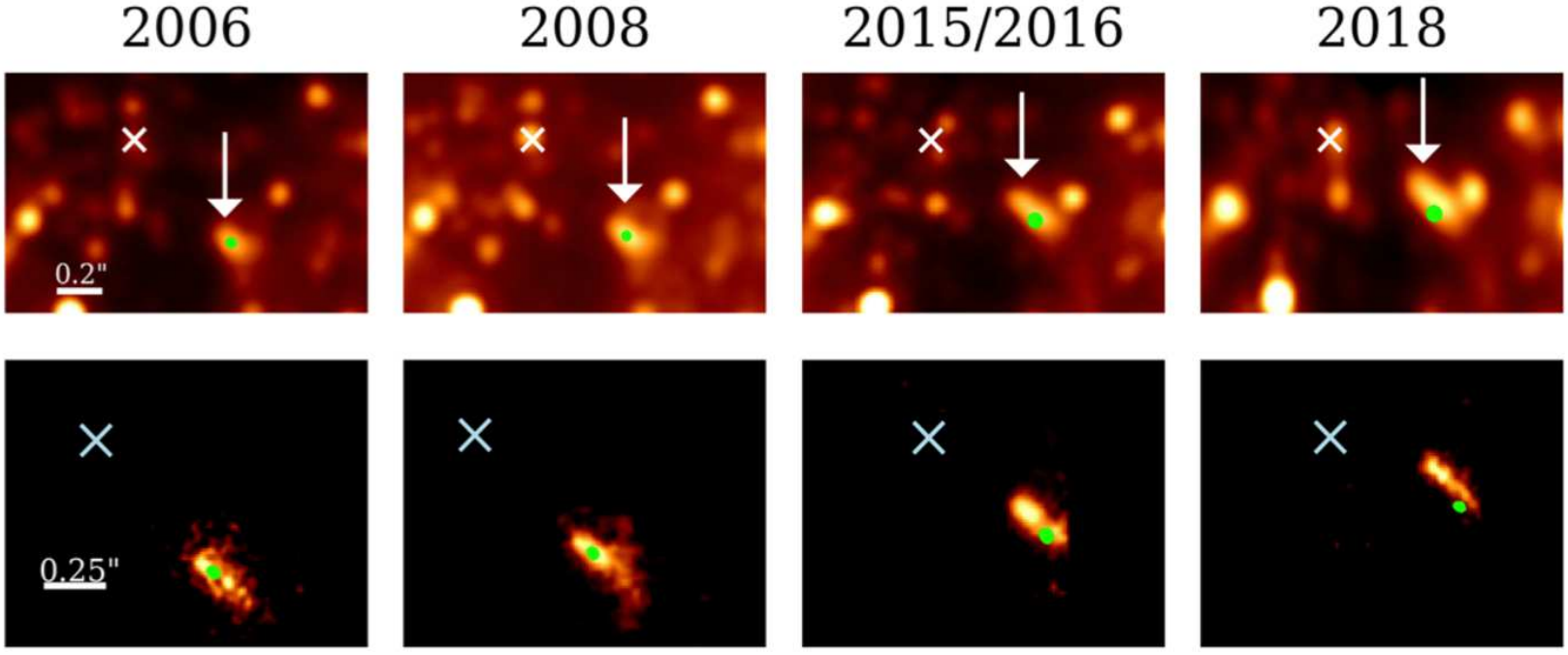


**Figure 5.** NACO $L'$-band continuum images (upper row) and SINFONI Doppler-shifted Br$\gamma$ line maps (lower row) displaying the immediate environment of Sgr A*.

# EMRI vs. TDE

The Astrophysical Journal, 909:62 (19pp), 2021 March 1 https://doi.org/10.3847/1538-4357/abd9c6


## First Observed Interaction of the Circumstellar Envelope of an S-star with the Environment of Sgr A*

Florian Peißker[1], ... Vladimír Karas[4], ...
[1] I. Phys... ...oeln.de
[5] LESIA, Observatoi... ...95 Meudon, France

The Astrophysical Journal, 909:62 (19pp), 2021 March 1

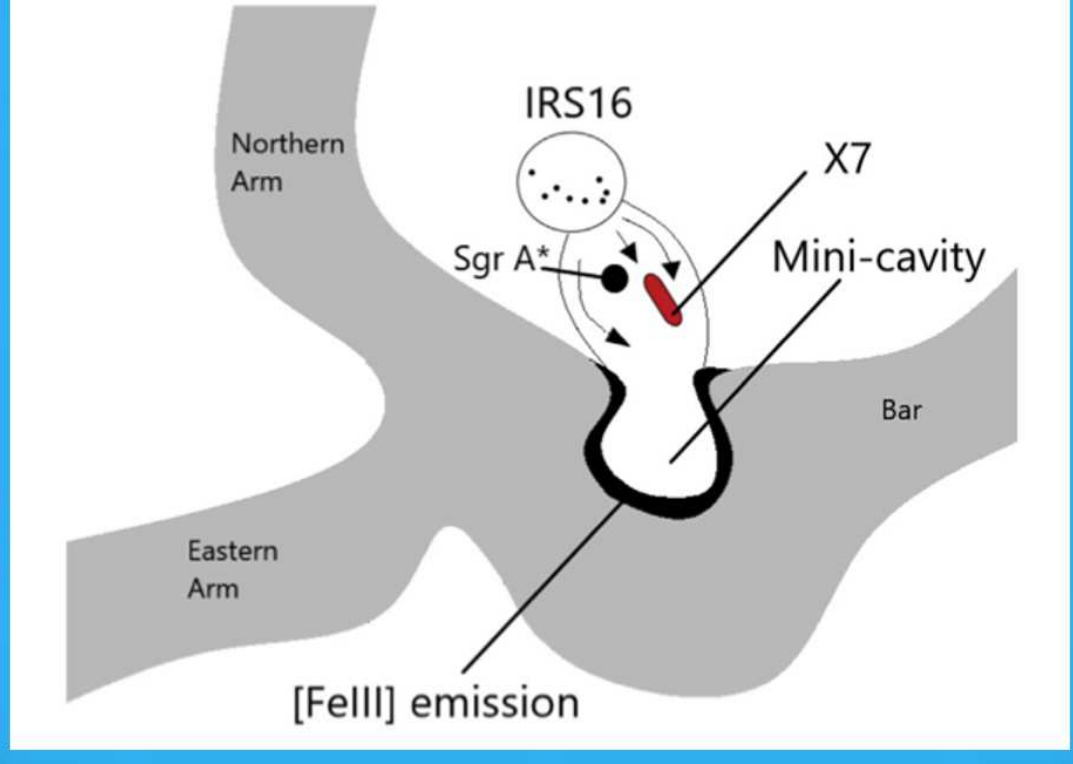





**Figure 5.** NACO $L'$-band continuum images (upper row) and SINFONI Doppler-shifted Br$\gamma$ line maps (lower row) displaying the immediate environment of Sgr A*.

# EMRI vs. TDE

## Millihertz oscillations near the innermost orbit of a supermassive black hole

Megan Masterson, Erin Kara, Christos Panagiotou, William N. Alston, Joheen Chakraborty, Kevin Burdge, Claudio Ricci, Sibasish Laha, Iair Arcavi, Riccardo Arcodia, S. Bradley Cenko, Andrew C. Fabian, Javier A. García, Margherita Giustini, Adam Ingram, Peter Kosec, Michael Loewenstein, Eileen T. Meyer, Giovanni Miniutti, Ciro Pinto, Ronald A. Remillard, Dev R. Sadaula, Onic I. Shuvo, Benny Trakhtenbrot & Jingyi Wang

*Nature* **638**, 370–375 (2025) | Cite this article

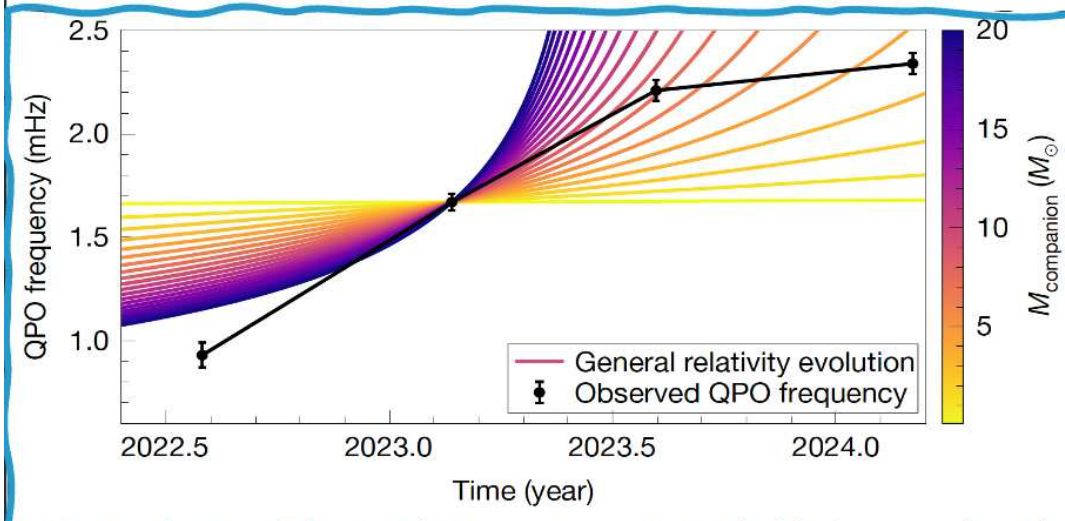


**Fig. 3 | Evolution of the QPO frequency over time.** The black points show the observed QPO frequency and 1$\sigma$ error bars, obtained by fitting an additional Lorentzian for the QPO. The coloured lines show the expected evolution of an extreme-mass-ratio companion under general relativity alone, assuming a circular orbit (eccentricity of $e = 0$) and companion masses ranging from 0.1 $M_\odot$ to 20 $M_\odot$. The colour bar shows the mass distribution. The general relativity model was chosen to match the QPO frequency in February 2023, as these were the data with the most significant detection and the lowest uncertainty on the QPO frequency. General relativity alone for an orbiting companion cannot account for the frequency evolution seen in 1ES 1927+654.

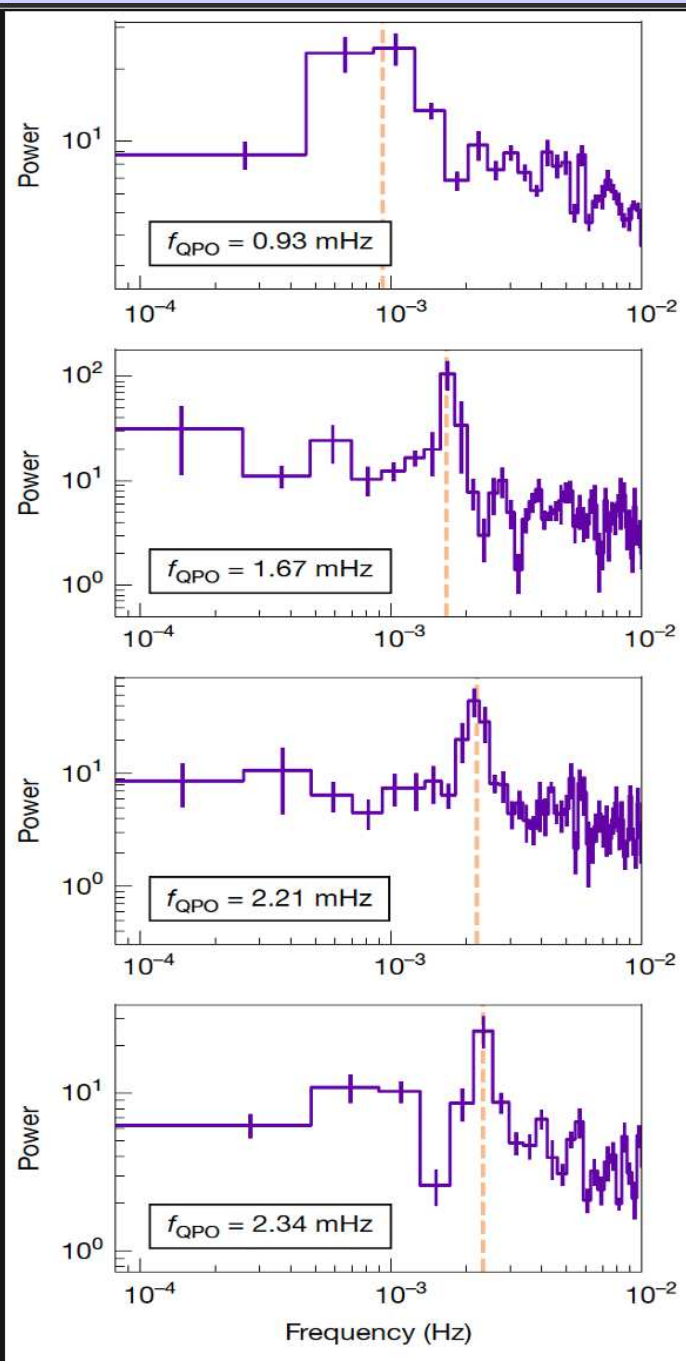

# *Thank you!*

## References


- Gravitating discs around black holes
  (Karas, Huré, Semerák, 2004, CQG 21, 1;
  Karas & Šubr, 2010, IAU Symp. 267, 332)
- Star-disc interactions in a galactic centre and oblateness of the inner stellar cluster
  (Šubr, Karas, Huré, 2004, MNRAS 345, 1177)
- Kozai oscillations acting together with dissiptive drag of a gaseous disc — transporting S-stars toward the centre
  (Šubr & Karas, 2005, A&A 433, 405)
- Stellar tidal disruptions due to the eccentricity oscillations
  (Karas & Šubr, 2007, A&A 470, 11)

# Discussion slides – Eccentric mergers

## AGN as potential factories for eccentric black hole mergers

Nature | Vol 603 | 10 March 2022 | 237

https://doi.org/10.1038/s41586-021-04333-1

Received: 8 October 2020

J. Samsing[1]✉, I. Bartos[2], D. J. D'Orazio[1], Z. Haiman[3], B. Kocsis[4,5], N. W. C. Leigh[6,7], B. Liu[1], M. E. Pessah[1] & H. Tagawa[8]

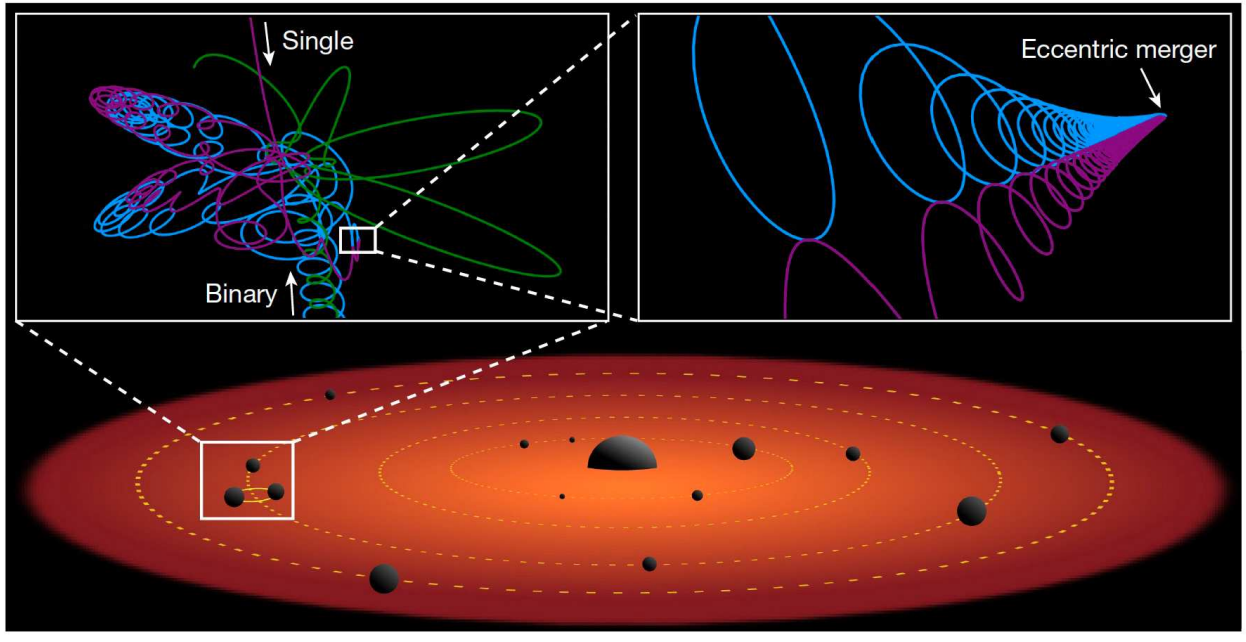


**Fig. 1 | Illustration of an eccentric LIGO-Virgo source forming in an AGN disk.** Bottom, AGN disk (not to scale) with its central supermassive black hole and a population of smaller orbiting black holes. These smaller black holes occasionally pair up to form binary black holes, which often undergo scatterings with the single-black-hole population. Top, outcome of a [50 $M_\odot$, 80 $M_\odot$] binary black hole interacting with an incoming [70 $M_\odot$] black hole, which results in a [80 $M_\odot$, 70 $M_\odot$] binary black hole merger during the interaction, with an eccentricity of about 0.5 in LIGO-Virgo.

# Case of subgiant star stripped to its helium core



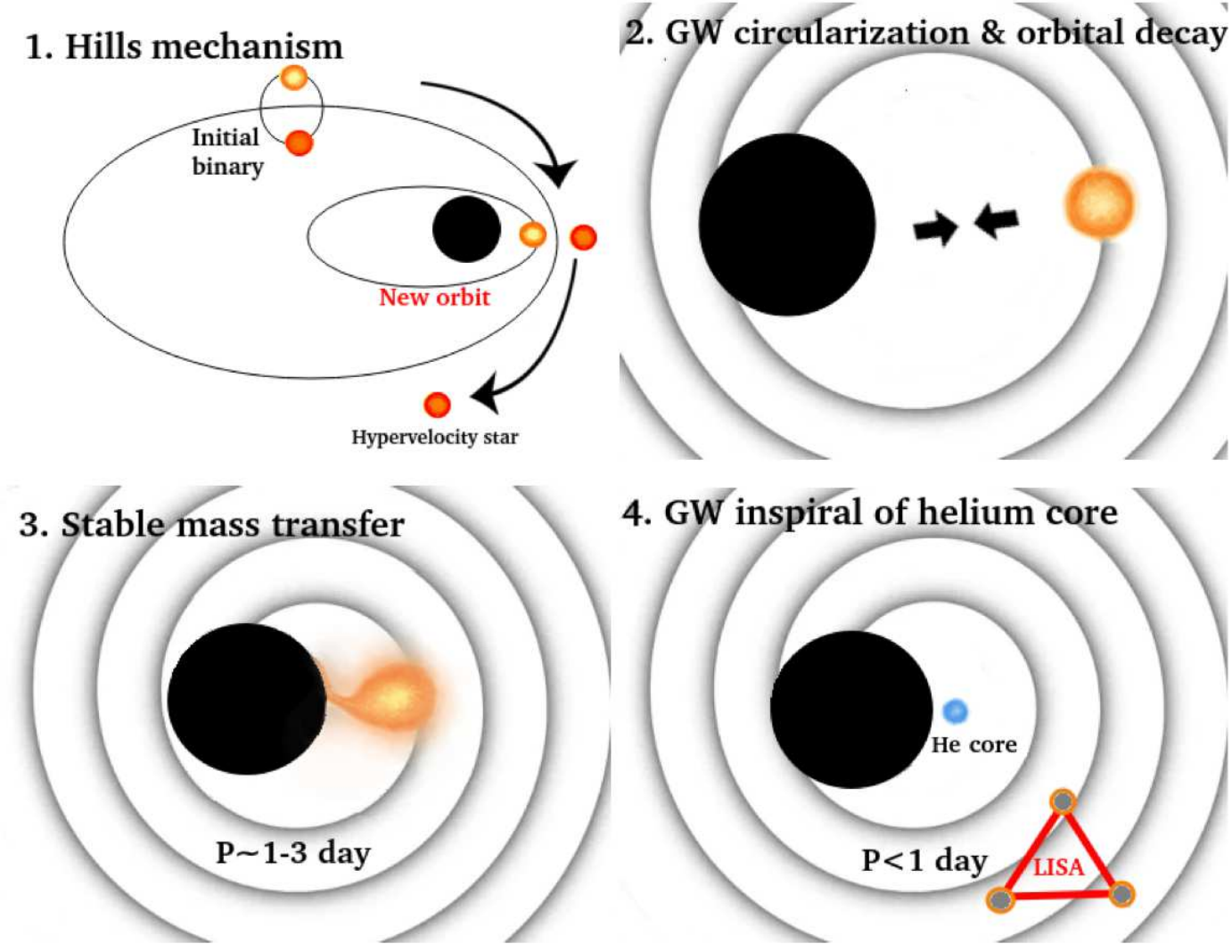


**Figure 1.** Cartoon representation of four relevant evolutionary stages of the system. Top left panel: the initial binary star system enters the Hill sphere of an SMBH and is disrupted. One star becomes gravitationally bound to the SMBH in an eccentric orbit, while the other is ejected from the Galactic nucleus, becoming a hypervelocity star. Top right panel: the orbit of the star bound to the SMBH gradually shrinks and circularizes owing to the strong emission of GWs. Bottom left panel: as the orbit continues to tighten, a subgiant star fills its Roche lobe, initiating a phase of long, stable mass transfer onto the SMBH. Bottom right panel: the star is eventually stripped of its hydrogen envelope during the mass transfer process. The system continues to shrink owing to GW emission, eventually entering the LISA frequency band as a detectable GW source.

# Evolution of tidal debris

The Astrophysical Journal, 904:99 (15pp), 2020 December 1 https://doi.org/10.3847/1538-4357/abb3cd


**Tidal Disruptions of Main-sequence Stars. II. Simulation Methodology and Stellar Mass Dependence of the Character of Full Tidal Disruptions**

Taeho Ryu[1], Julian Krolik[1], Tsvi Piran[2], and Scott C. Noble[3]
[1] Physics and Astronomy Department, Johns Hopkins University, Baltimore, MD 21218, USA; tryu2@jhu.edu
[2] Racah Institute of Physics, Hebrew University, Jerusalem 91904, Israel
[3] Gravitational Astrophysics Laboratory, Goddard Space Flight Center, Greenbelt, MD 20771, USA
*Received 2019 July 26; revised 2020 April 10; accepted 2020 July 14; published 2020 November 25*

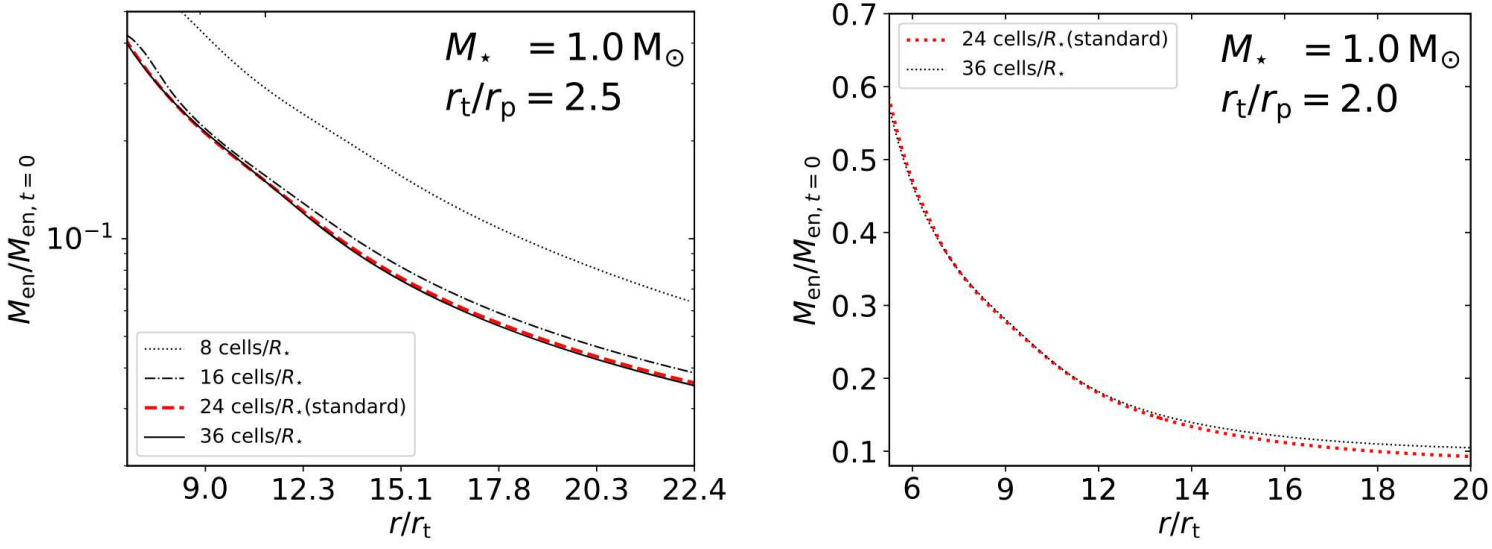


**Figure 11.** Evolution, as the stellar debris move away from the SMBH, of mass enclosed in the computational domain $M_{en}$, relative to its initial mass $M_{en,t=0}$, for full (the left panel, $r_t/r_p = 2.5$) and partial (the right panel, $r_t/r_p = 2.0$) TDE simulations ($M_\star = 1$, $M_{BH} = 10^6$) with different resolutions. The red dashed line represents the standard resolution of 24 cells per $R_\star$.

# Example: S2-star

Classification:

- O9 main-sequence star
- $M_* \approx 15 M_\odot$
- age $\lesssim 10\mathrm{Myr}$

Kinematics:

- $P = 15.8\,\mathrm{yr}$
- $a = 2.5 \times 10^4 R_\mathrm{g}$
- $e = 0.87$
- $i = -47.3°$

Puzzle: Too young to be there

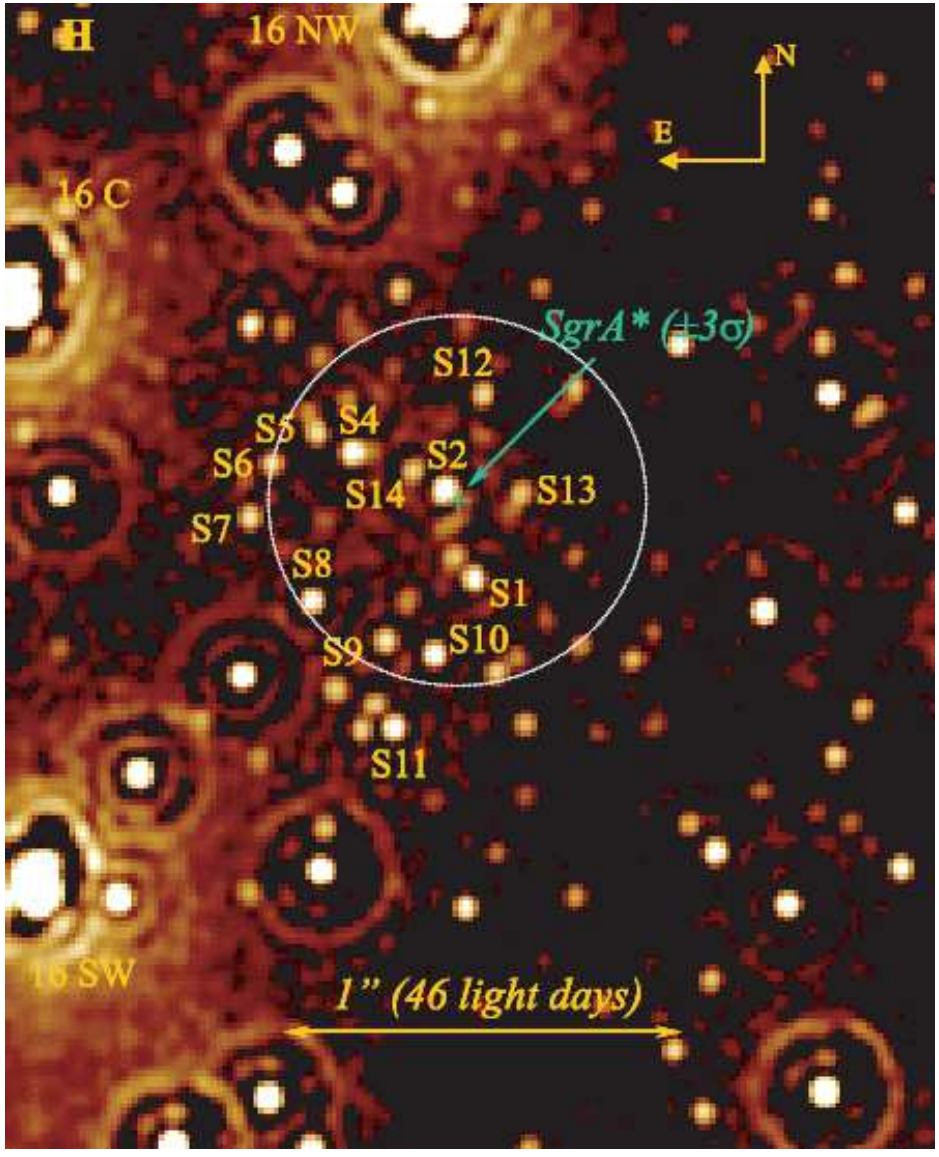

# *Kozai resonance mechanism*

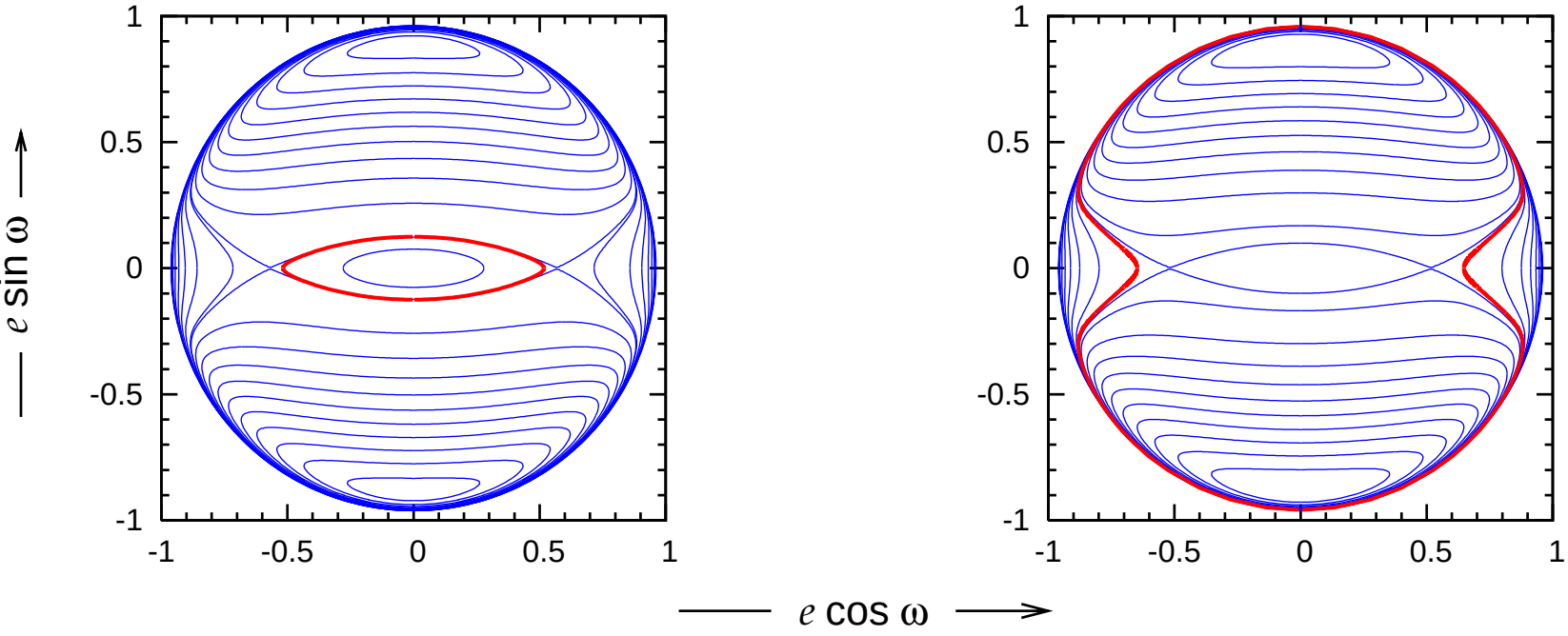

# Temporal evolution